

# Effects of cobalt replacement by nickel, manganese, aluminium and iron on the crystallographic and electrochemical properties of AB<sub>5</sub>-type alloys

S. Vivet<sup>a,\*</sup>, J.-M. Joubert<sup>a</sup>, B. Knosp<sup>a,b</sup>, A. Percheron-Guégan<sup>a</sup>

<sup>a</sup>Laboratoire de Chimie Métallurgique des Terres Rares, ISCSA, CNRS, 2–8 Rue H. Dunant, 94320 Thiais Cedex, France

<sup>b</sup>SAFT, Direction de la Recherche, 111 Bd Alfred Daney, 33074 Bordeaux Cedex, France

Received 3 September 2002; accepted 6 December 2002

## Abstract

Cobalt has been partially or totally replaced by other elements such as Ni, Mn, Al or Fe in MmNi<sub>4.07</sub>Mn<sub>0.63</sub>Al<sub>0.2</sub>Co<sub>0.4</sub> composition in order to evaluate the effects on microstructure and electrochemical properties (capacity, cycle life, corrosion . . .). The cycle life of the electrodes for which cobalt has been replaced by nickel or manganese is strongly diminished. However, interestingly, Fe-containing electrodes behave as well as Co-containing electrodes in terms of cycle life, despite a slight capacity reduction. Moreover, the SEM picture revealed that in a similar way to Co, Fe reduces the alloy pulverisation during cycling. This result is in agreement with a low discrete lattice expansion for these Fe-containing alloys.

© 2003 Elsevier B.V. All rights reserved.

**Keywords:** Intermetallics; Hydrogen storage materials; X-Ray diffraction; Electrochemical reactions

## 1. Introduction

The standard AB<sub>5</sub> composition used for metal hydride electrodes in Ni–MH batteries is MmNi<sub>3.55</sub>Mn<sub>0.4</sub>Al<sub>0.3</sub>Co<sub>0.75</sub> (A=Mm for mischmetal, a mixture of rare earth; B=Ni, Mn, Al and Co) [1,2]. The presence of cobalt allows one to enhance the cycle life possibly due to the reduction of the lattice expansion occurring during the hydrogen absorption [1,3–5]. However, cobalt is expensive and drastically increases the total alloy cost. Therefore, many works have been carried out in order to reduce its content. This was achieved recently by Cocciantelli et al. [6] who have shown that increasing the stoichiometry (ratio B/A) from 5 to 5.3 allows one to reduce the cobalt rate from 10% (0.75Co/AB<sub>5</sub>) to 5% in weight (0.40Co/AB<sub>5.3</sub>) without a significant decrease of the cycle life. In the present work, the effects of a further decrease of the cobalt rate are investigated by means of partial or total replacement of cobalt by other elements. The crystallographic and electrochemical properties of (Mm)-based alloys with the composition of MmNi<sub>4.07</sub>Mn<sub>0.63</sub>Al<sub>0.2</sub>Co<sub>0.4-x</sub>M<sub>x</sub> ( $x=0$ ,  $x=0.25$ ,  $x=0.4$ , M=Ni, Mn, Al, Fe) were examined.

\*Corresponding author. Tel.: +33-1-4978-1207; fax: +33-1-4978-1203.

E-mail address: [sonia.vivet@glvt-cnrs.fr](mailto:sonia.vivet@glvt-cnrs.fr) (S. Vivet).

## 2. Experimental

### 2.1. Preparation and characterisation of the alloys

The alloys were prepared by melting the pure elements (La, Ce, Nd, Pr: 99.9%; Ni: 99.95%; Mn, Co: 99.99%; Al: 99.9%; Fe: 99.98%) in an induction furnace on a water-cooled copper crucible under a secondary vacuum. They were annealed in order to obtain good homogeneity, single phase character and have been characterised by optical microscopy, electron probe microanalysis (EPMA) and powder X-ray diffraction (XRD). The pressure–composition isotherm curves were measured with a Sievert's type apparatus at 40 °C by absorption of H<sub>2</sub> gas. In order to measure the discrete lattice expansion [ $\Delta V/V=(V_{\beta}-V_{\alpha})/V_{\alpha}$ ] occurring during the transition from  $\alpha$  to  $\beta$  hydride, XRD has been used on partially hydrogenated samples.

### 2.2. Electrochemical measurement

Each electrode was prepared by mixing alloy powder (<63  $\mu\text{m}$ ) with a PTFE suspension and nickel powder in the weight ratio of 65% alloy, 30% Ni powder, 5% PTFE. The mixture was then mechanically pressed onto a nickel grid attached to a nickel connection. Cells consisted of a negative electrode and two positive foam electrodes iso-

lated from each other by a polyolefine separator. 8.7 M KOH aqueous solution is used as electrolyte.

After a preliminary charge at  $C/10$  (30 mA/g) for 2 h, cells were stored during 3 h at 70 °C in order to remove surface oxide. For the 10 activation cycles and discharge capacity, the electrodes were submitted to 16 h charge at  $C/10$  rate, 1 h rest and discharge at  $C/5$  rate (60 mA/g) down to 0.9 V cut-off voltage. Accelerated cycling between discharge capacities measurements were carried out at  $C$  rate (300 mA/g) for 48 min in discharge and 52 min in charge.

### 3. Results

Compositions correspond to the formula  $MmNi_{4.07}Mn_{0.63}Al_{0.2}Co_{0.4-x}M_x$  with  $x=0$  (5 wt.% Co),  $x=0.25$  (2 wt.% Co),  $x=0.4$  (0 wt.% Co) and  $M=Ni, Mn, Al, Fe$ . Stoichiometry (B/A ratio) is 5.3 and the mischmetal is La enriched ( $Mm=La_{0.7}Ce_{0.22}Nd_{0.06}Pr_{0.02}$ ). Table 1 presents the results of the metallurgical characterisation of the alloys, labelled by  $M_n$  with  $M$  the substituted element and  $n$  the cobalt weight percent rate.

In  $Al_2$  and  $Al_0$  alloys, precipitation of an f.c.c. secondary phase is observed (<2 wt.%) in agreement with the measured stoichiometry of the main phase (5.18 and 5.06, respectively) showing that aluminium content displaces the homogeneity range limit towards lower B/A ratio. Moreover, the X-ray diffraction pattern of  $Ni_0$  shows unexpected peak shouldering. This was attributed to the presence of two distinct  $CaCu_5$  phases with slightly different compositions and lattice parameters ( $a_1=5.011$  Å,  $c_1=4.069$  Å for main phase and  $a_2=5.013$  Å,  $c_2=4.050$  Å). Higher  $a$  and lower  $c$  values for the second phase indicates a smaller B/A ratio for this phase. Other samples show single phase character and analysed composition close to nominal with a B/A ratio close to 5.3. Cell volumes plotted in Fig. 1 are in agreement with the atomic radii of the substituted elements.

The pressure–composition isotherms measured at 40 °C

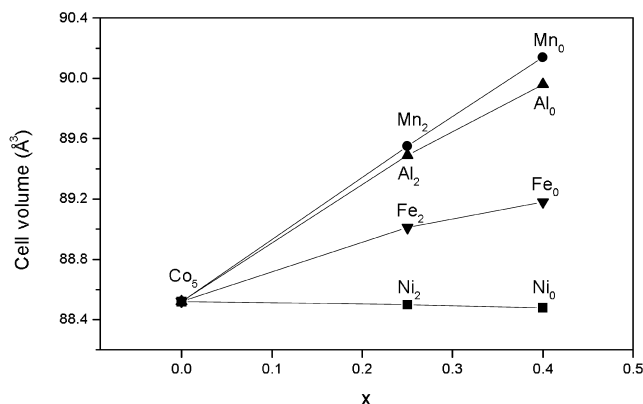


Fig. 1. Unit cell volume as a function of  $x$  in  $MmNi_{4.07}Mn_{0.63}Al_{0.2}Co_{0.4-x}M_x$  alloys.

are presented in Fig. 2 and the experimental values are listed in Table 2. Highest solid–gas capacities are observed for Ni-rich compounds and Co-containing compounds. On the contrary, total substitution of cobalt by aluminium and iron induces capacity decreases of 4.7 and 3%, respectively. In Al-rich compounds, this decrease is explained by the precipitation of an f.c.c. secondary phase which does not absorb hydrogen and by the presence of aluminium which is known to decrease hydrogen capacity [7]. Plateau pressure decrease when Co is substituted by Fe, Mn and Al is consistent with the observed cell volume increase.

X-Ray diffraction on partially hydrogenated Ni-rich samples ( $Ni_0$  and  $Ni_2$ ) reveals two alpha and two beta phases coexisting. This result concurs with the presence of two  $CaCu_5$  phases observed by X-ray diffraction measurements on  $Ni_0$  intermetallic compound and suggests that the same behaviour occurs in  $Ni_2$  sample. X-Ray diffraction on samples partially hydrogenated shows that the lattice expansion is strongly reduced for Fe-containing alloys.

The discharge capacity of the  $MmNi_{4.07}Mn_{0.63}Al_{0.2}Co_{0.4-x}M_x$  electrode as a function of cycle number is shown in Fig. 3. The highest discharge capacities are obtained when cobalt is substituted partially or totally by nickel or manganese, but the cycle life is diminished. Substitution of cobalt by aluminium yields not

Table 1  
Metallurgical characterisation of the alloys

Reference	x	Alloy	XRD			EPMA		
			Cell parameters		Volume (Å <sup>3</sup> )	Second phases	B/A ratio	Second phases (at.%)
			a (Å)	c (Å)				
Co <sub>5</sub>	0	$MmNi_{4.07}Mn_{0.63}Al_{0.2}Co_{0.4}$	5.015	4.063	88.52	–	5.28	–
Ni <sub>2</sub>	0.25	$MmNi_{4.32}Mn_{0.63}Al_{0.2}Co_{0.15}$	5.013	4.066	88.50	–	5.28	–
Mn <sub>2</sub>	0.25	$MmNi_{4.07}Mn_{0.88}Al_{0.2}Co_{0.15}$	5.031	4.086	89.55	–	5.23	–
Al <sub>2</sub>	0.25	$MmNi_{4.07}Mn_{0.63}Al_{0.45}Co_{0.15}$	5.032	4.081	89.49	–	5.18	$Ni_{52}Mn_{27}Al_{19}Co_2$
Fe <sub>2</sub>	0.25	$MmNi_{4.07}Mn_{0.63}Al_{0.2}Fe_{0.25}Co_{0.15}$	5.023	4.073	89.01	–	5.30	–
Ni <sub>0</sub>	0.4	$MmNi_{4.47}Mn_{0.63}Al_{0.2}$	5.011	4.069	88.48	AB <sub>5</sub> (39%)	5.34	–
Mn <sub>0</sub>	0.4	$MmNi_{4.07}Mn_{1.03}Al_{0.2}$	5.042	4.093	90.14	–	5.17	–
Al <sub>0</sub>	0.4	$MmNi_{4.07}Mn_{0.63}Al_{0.6}$	5.044	4.083	89.96	Ni fcc (4%)	5.06	$Ni_{53}Mn_{25}Al_{22}$
Fe <sub>0</sub>	0.4	$MmNi_{4.07}Mn_{0.63}Al_{0.2}Fe_{0.4}$	5.026	4.076	89.18	–	5.26	–

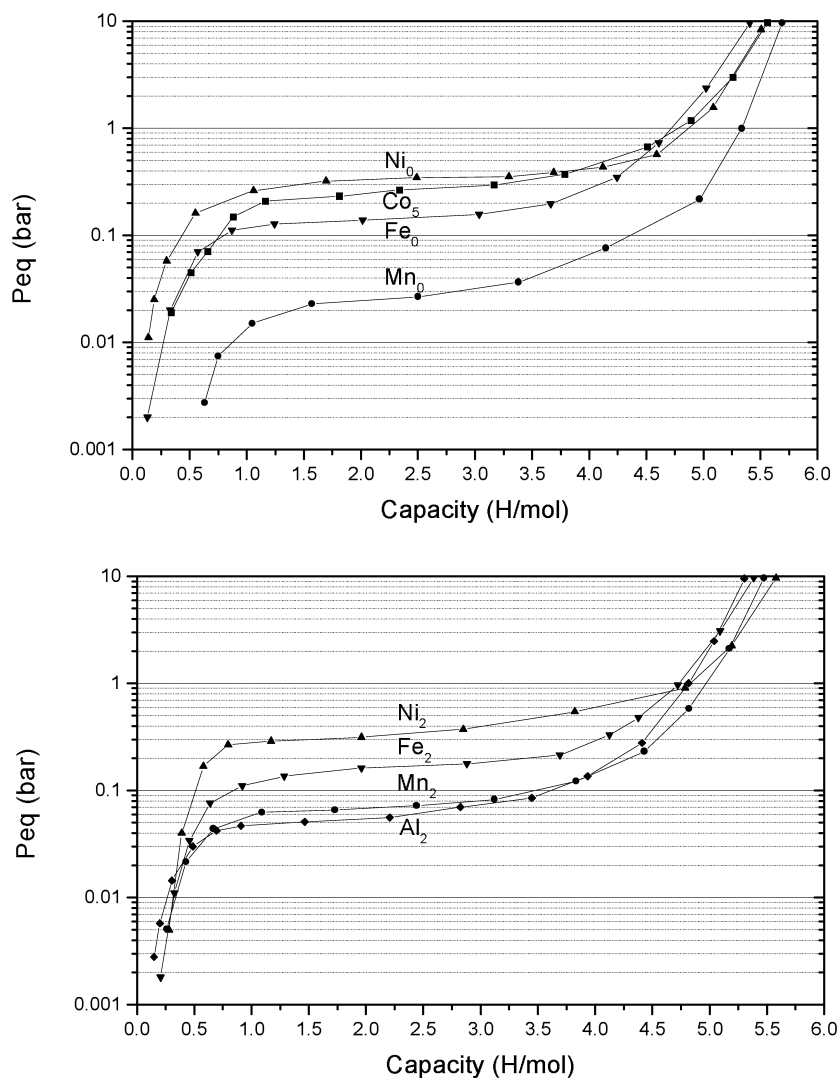
Fig. 2. Desorption isotherm at 40 °C for  $\text{MmNi}_{4.07}\text{Mn}_{0.63}\text{Al}_{0.2}\text{Co}_{0.4-x}\text{M}_x$  compounds.

Table 2

Data obtained from hydrogen pressure–composition isotherms and electrochemical measurements for  $\text{MmNi}_{4.07}\text{Mn}_{0.63}\text{Al}_{0.2}\text{Co}_{0.4-x}\text{M}_x$  compounds

Reference	Alloys	$P_{\text{abs}}^a$ (bar)	$P_{\text{des}}^b$ (bar)	$C_{\text{sg}}^c$ (H/mol $\text{AB}_{5.3}$ )	$C_{\text{sg}}^d$ (mAh/g)	$\Delta V/V^e$ (%)	$C_{\text{el}}^f$ (mAh/g)	$C_{200}/C_{\text{el}}^g$ (%)
Co <sub>5</sub>	$\text{MmNi}_{4.07}\text{Mn}_{0.63}\text{Al}_{0.2}\text{Co}_{0.4}$	0.37	0.27	5.56	337	10.46	295	97
Ni <sub>2</sub>	$\text{MmNi}_{4.32}\text{Mn}_{0.63}\text{Al}_{0.2}\text{Co}_{0.15}$	0.39	0.35	5.58	338	10.3/15.4	304	94
Mn <sub>2</sub>	$\text{MmNi}_{4.07}\text{Mn}_{0.88}\text{Al}_{0.2}\text{Co}_{0.15}$	0.08	0.07	5.47	332	10.70	298	92
Al <sub>2</sub>	$\text{MmNi}_{4.07}\text{Mn}_{0.63}\text{Al}_{0.45}\text{Co}_{0.15}$	0.07	0.06	5.30	327	10.45	284	93
Fe <sub>2</sub>	$\text{MmNi}_{4.07}\text{Mn}_{0.63}\text{Al}_{0.2}\text{Fe}_{0.25}\text{Co}_{0.15}$	0.19	0.17	5.38	327	9.07	286	94
Ni <sub>0</sub>	$\text{MmNi}_{4.47}\text{Mn}_{0.63}\text{Al}_{0.2}$	0.39	0.35	5.51	334	11.9/17.4	297	87
Mn <sub>0</sub>	$\text{MmNi}_{4.07}\text{Mn}_{1.03}\text{Al}_{0.2}$	0.04	0.03	5.60	340	12	293	78
Fe <sub>0</sub>	$\text{MmNi}_{4.07}\text{Mn}_{0.63}\text{Al}_{0.2}\text{Fe}_{0.4}$	0.17	0.15	5.40	328	8.81	282	95

<sup>a</sup> Absorption pressure.<sup>b</sup> Desorption pressure.<sup>c</sup> Solid–gas capacity measured under 10 bar of hydrogen gas.<sup>d</sup> Solid–gas capacity converted into electrochemical units.<sup>e</sup> Volumic discrete lattice expansion occurring during the formation of the hydride phase.<sup>f</sup> Maximal discharge capacity obtained by electrochemical measurements.<sup>g</sup> Capacity after 200 cycles divided by the maximal discharge capacity.

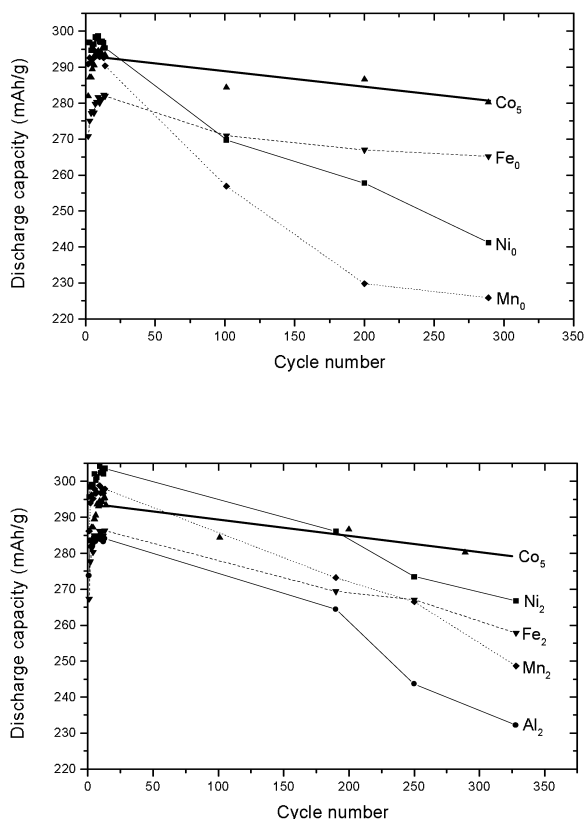
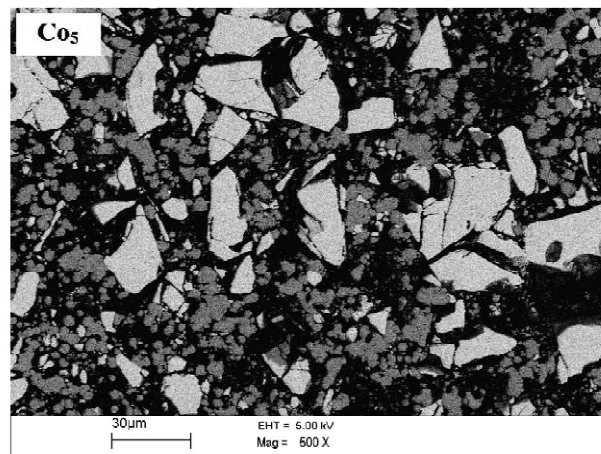


Fig. 3. Discharge capacity as a function of cycle number for the  $\text{MmNi}_{4.07}\text{Mn}_{0.63}\text{Al}_{0.2}\text{Co}_{0.4-x}\text{M}_x$  ( $x=0.25$ ,  $x=0.4$ ) electrodes.

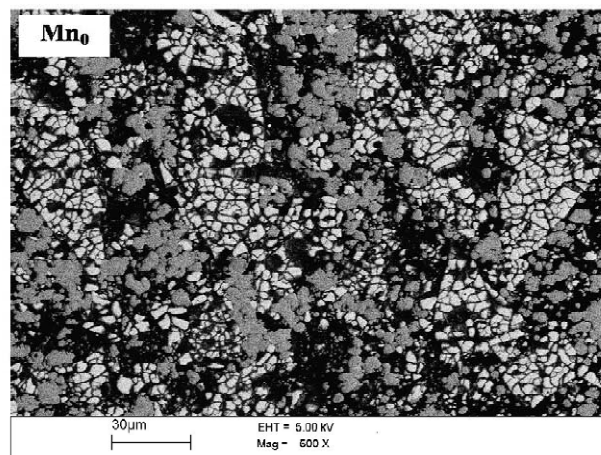
only a strong discharge capacity decrease but also a cycle life decrease (capacity loss about 18% between 13th cycle and 330th cycle for  $\text{Al}_2$  alloy). However, interestingly Fe-containing electrodes behave as well as Co-containing electrodes in terms of cycle life despite a slight initial capacity reduction about 5%. Scanning electron microscopy (SEM) pictures of  $\text{MmNi}_{4.07}\text{Mn}_{0.63}\text{Al}_{0.2}\text{M}_{0.4}$  ( $M=\text{Co}$ ,  $\text{Mn}$ ,  $\text{Fe}$ ) cycled electrodes (Fig. 4) revealed that, in a similar way to cobalt, iron reduces the alloy pulverisation. After 300 cycles, the effect of the pulverisation of  $\text{MmNi}_{4.07}\text{Mn}_{0.63}\text{Al}_{0.2}\text{M}_{0.4}$  ( $M=\text{Mn}$ ) is noticeable (grain size =  $5\ \mu\text{m}$ ) while, for Fe and Co-containing alloys the pulverization is scarcely observed (grain size =  $15\text{--}20\ \mu\text{m}$ ).

#### 4. Discussion and conclusion

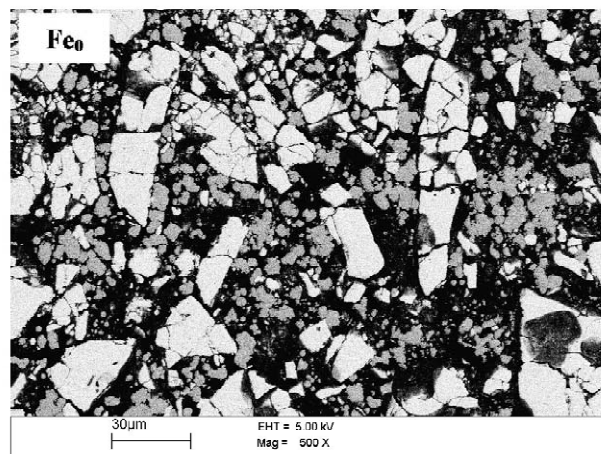
Alloys corresponding to the general formula  $\text{MmNi}_{4.07}\text{Mn}_{0.63}\text{Al}_{0.2}\text{Co}_{0.4-x}\text{M}_x$  with  $x=0$  (5 wt.% Co),  $x=0.25$  (2 wt.% Co),  $x=0.4$  (0 wt.% Co) and  $M=\text{Ni}$ ,  $\text{Mn}$ ,  $\text{Al}$ ,  $\text{Fe}$  were elaborated in order to evaluate the effects of composition changes on the electrochemical properties (capacity, cycle life, corrosion...). For Ni-rich alloys ( $\text{Ni}_0$  and  $\text{Ni}_2$ ), two distinct  $\text{CaCu}_5$  phases are present in spite of annealing, one of which having a lower stoichiometry. In



(A)



(B)



(C)

Fig. 4. SEM micrographs after 300 electrochemical charge/discharge cycles of  $\text{MmNi}_{4.07}\text{Mn}_{0.63}\text{Al}_{0.2}\text{Co}_{0.4-x}\text{M}_x$  electrode (A)  $x=0$ , (B)  $x=0.4$ ,  $M=\text{Mn}$ , (C)  $x=0.4$ ,  $M=\text{Fe}$ .

$Al_0$  and  $Al_2$  compounds, the high aluminium content lowers the over stoichiometric range and induces the presence of a second phase. Alloys in which cobalt has been substituted by iron and manganese show single phase character and a B/A ratio close to 5.3. Maximal discharge capacities obtained by electrochemical measurements are in agreement with solid–gas capacity. These two techniques show a capacity lowering of about 3 to 4% when cobalt is substituted by iron or aluminium. This reduction of the amount of hydrogen absorbed is also observed in ternary  $LaNi_{5-x}Fe_x$  [8] and  $LaNi_{5-x}Al_x$  [7] and is explained by a reduction in the number of occupied sites ( $6m$ ,  $12n$ ,  $4h$ ). In our case, the capacity lowering of  $Al_0$  and  $Al_2$  is also ascribed to the presence of the secondary phase.

While the role of the second  $CaCu_5$  phase in  $Ni_0$  and  $Ni_2$  on the cycle life properties can hardly be evaluated, it is clear that cobalt replacement by manganese and aluminium drastically reduce the cycle life. As this replacement does not involve any major change of the discrete lattice expansion, it shows that not only this latter parameter is relevant. However, the partial or total replacement of cobalt by iron leads to a similar cycle life as the one of Co-containing alloys. The discrete lattice expansion ( $\Delta V/V$ ) is strongly reduced for Fe-containing alloys and SEM pictures after cycling show the beneficial effect of iron on decrepitation correlated with cycle life. This beneficial effect of a partial substitution of cobalt by iron on cycle life has been already observed in stoichiometric alloys [9,10]. According to Züttel et al. [9], the excellent cyclic stability of iron containing alloys cannot be explained only with their small volume expansion but other important factors must be taking into account such as alloy hardness, final grain size distribution and the formation of protecting surface oxide layers. Hasegawa et al. [11] explain this excellent electrode characteristics by a transition metal layer formation composed of Co, Fe and Ni on the alloy surface. According to them, this layer has a catalytic activity and the function of inhibiting alloy corrosion.

In this work, we have shown that a total substitution of cobalt is possible without significant capacity loss during cycling using Fe-rich compounds and a stoichiometry of 5.3. Iron is known to poison the positive electrode [12,13]. However, measurements have shown that dissolved iron precipitates in the negative electrode [14]. Consequently,

no detrimental effect on the positive electrode capacity was observed using iron containing alloys [10].

Development of Co-free electrodes is the major challenge for industrial low cost development of Ni–MH batteries. Iron, which is relatively inexpensive, could be used to replace expensive cobalt entirely or partly in Ni–MH secondary cell but improvement are still needed in terms of capacity.

### Acknowledgements

The authors would like to thank E. Leroy for electron probe microanalysis, J.-L. Pastol for SEM observation and V. Ducours for electrochemical measurement follow-up. S.V. wishes to acknowledge ADEME for financial support.

### References

- [1] H. Ogawa, M. Ikoma, H. Kawano, I. Matsumoto, J. Power Sources 12 (1988) 393.
- [2] M. Ikoma, H. Kawano, I. Matsumoto, N. Yanagihara, Eur. Pat. No. 0271043 (1987).
- [3] J.J.G. Willems, K.H.J. Buschow, J. Less-Common Met. 129 (1987) 13.
- [4] T. Sakai, K. Oguro, H. Miyamura, N. Kuriyama, A. Kato, H. Ishikawa, J. Less-Common Met. 161 (1990) 193.
- [5] G.D. Adzic, J.R. Johnson, S. Mukerjee, J.M. Breen, J.J. Reilly, J. Alloys Comp. 253–254 (1997) 579.
- [6] J.-M. Cocciantelli, C. Arquey, A. Percheron-Guégan, Brevet Français No. FR 9709568 (1997).
- [7] H. Diaz, A. Percheron-Guégan, J.-C. Achard, C. Chatillon, J.-C. Mathieu, Int. J. Hydrogen Energy 4 (1979) 445.
- [8] J. Lamloumi, A. Percheron-Guégan, C. Lartigue, J.-C. Achard, G. Jehanno, J. Less-Common Met. 130 (1987) 111.
- [9] A. Züttel, D. Chartouni, K. Gross, P. Spatz, M. Bächler, F. Lichtenberg, A. Fölzer, N.J.E. Adkins, J. Alloys Comp. 253–254 (1997) 626.
- [10] J.-M. Cocciantelli, P. Bernard, S. Fernandez, J. Atkin, J. Alloys Comp. 253–254 (1997) 642.
- [11] K. Hasegawa, M. Ohnishi, M. Oshitani, K. Takeshima, Y. Matsu-  
maru, Z. Phys. Chem. 183 (1994) 325.
- [12] I. Krejčí, J. Mrha, B. Folkesson, R. Larsson, J. Power Sources 21 (1987) 77.
- [13] A. Kamnev, Electrochem. Acta 41 (1996) 267.
- [14] M. Ayari, V. Paul-Boncour, J. Lamloumi, A. Percheron-Guégan, J. Magn. Mater. 242–245 (2002) 850.